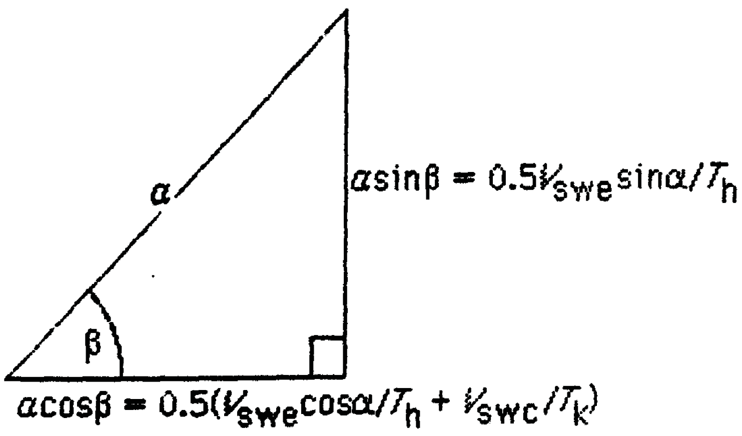

Figure 3.6 Trigonometric Substitution

Evaluating the mass of gas m_t always presents a little difficulty. It is never clear under which conditions it should be evaluated or how leakage may affect its value. A simple method of evaluating m_t follows which has been found to return acceptable results even the more sophisticated analyses [Be78, UB84].

Defining the mean cyclic pressure (also referred to as the charge pressure):

$$\langle p \rangle = 1/(2\pi)\oint m_t R[a\cos(\beta + \theta) + S]^{-1}d\theta$$

From standard integral tables [Pe61]:

$$\langle p \rangle = m_t R / \left[S\sqrt{1-(a/S)^2}\right]$$

which gives

$$m_t = \langle p \rangle S\sqrt{1-(a/S)^2}/R \tag{3.29}$$

Substitution of (3.29) into (3.28):

$$p = \langle p \rangle \sqrt{1-(a/S)^2}/[(a/S)\cos(\beta+\theta)+1] \tag{3.30}$$

In many cases $(a/S)^2 \ll 1$ and may therefore be neglected, thus

$$p \approx \langle p \rangle /[(a/S)\cos(\beta+\theta)+1] \tag{3.31}$$

(3.30) may also be expanded by Fourier series to arrive at

$$p = \langle p \rangle \Big[1 + 2(S/a)\big[\sqrt{1-(a/S)^2} - 1\big]\cos(\beta+\theta) + \big[\sqrt{1-(a/S)^2}(a/S)^2/2\big]\cos 2(\beta+\theta)\Big] \tag{3.32}$$

which indicates that pressure is approximately a harmonic variation with amplitude $2\langle p \rangle (S/a)\big[\sqrt{1-(a/S)^2} - 1\big]$ and phase β plus a second harmonic of much smaller amplitude. This is shown in Figure 3.7.

The cyclic work and heat transfer may now be evaluated from Equation (3.14).

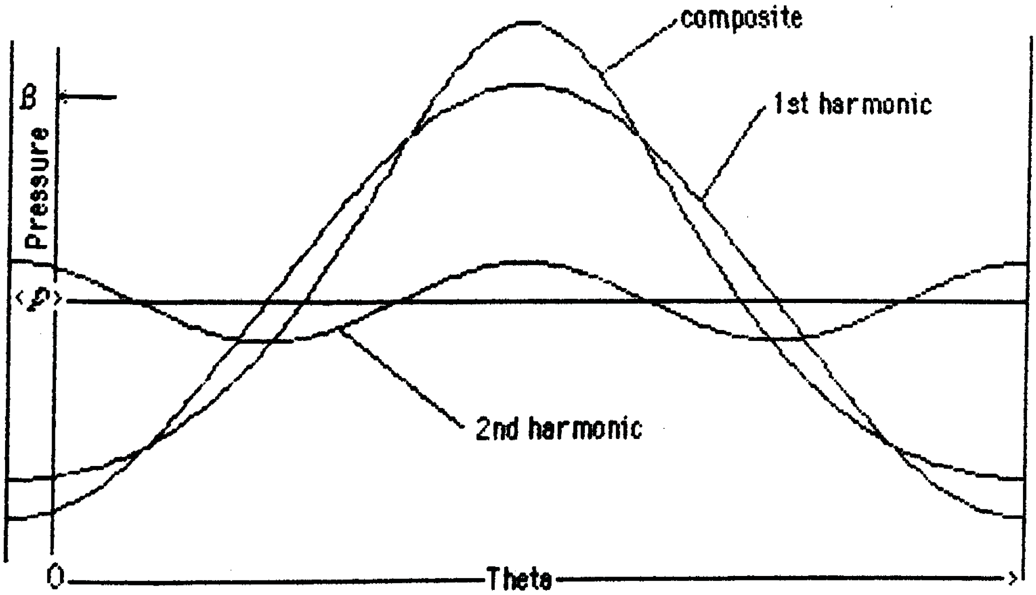

Figure 3.7 Isothermal Pressure Variation

For the compression space:

$$W_C = Q_C = \oint p \, d V_C$$

Substitution of Equation (3.30) and the result for $D V_C$ from Table 3.1 (noting that $D V_C = d V_C / dt$) into the above equation yields:

$$W_C = Q_C = -0.5 \langle p \rangle \sqrt{1 - (a/5)^2} \, V_{swc} \oint \sin\theta [(a/5)\cos(\beta + \theta) + 1]^{-1} d\theta \qquad (3.33)$$

The solution of (3.33) involves a certain amount of manipulation and has been solved many times in the literature; in approximate form [Wa73], and exact [Ur77, Be78, Wa80 and RH83]. The reader is referred to these references for the method of solution, in this work only the final solution is given. Thus the integration of (3.33) is

$$W_c = Q_c = \pi V_{swc} \langle p \rangle (S/a)[\sqrt{1-(a/S)^2} - 1]\sin\beta \tag{3.34}$$

By similar procedure, the result for the expansion space is

$$W_e = Q_e = \pi V_{swe} \langle p \rangle (S/a)[\sqrt{1-(a/S)^2} - 1]\sin(\beta - \alpha) \tag{3.35}$$

Both (3.34) and (3.35) are exact solutions.

The total work is simply $W_c + W_e$ and is given by

$$W = \pi \langle p \rangle (S/a)[\sqrt{1-(a/S)^2} - 1][V_{swc}\sin\beta + V_{swe}\sin(\beta - \alpha)] \tag{3.36}$$

and the power is

$$P = \omega/(2\pi)\, W = fW \tag{3.37}$$

where f is the frequency in Hertz.

The indicated efficiency follows

$$\eta = W/Q_e \tag{3.38}$$

From (3.36) and (3.35) the indicated efficiency reduces to

$$\eta = 1 - T_k/T_h \tag{3.39}$$

which is the Carnot efficiency as would be expected (Chapter 2).

Typically, one may expect a source temperature of around 1000K and a rejection temperature of 300K. This would therefore give an ideal efficiency of around 67%. Real thermodynamic effects degrade this value by about 30% in a well designed machine operating at peak efficiency [Wa80]. At the present state of the art it seems not unreasonable to expect an actual peak efficiency of around 47%, though some experimental automotive engines have attained indicated efficiencies of around 55%.

The results for power and efficiency thus far derived are the limit of Schmidt's original effort. Table 3.2 summarises the basic Schmidt equations for easy reference.

The Schmidt results are useful in obtaining an estimation of the power of an engine given its geometry and operating conditions. To size the heat exchangers, both the heat transfers and gas flow rates are required. In the following sections the Schmidt analysis is extended so as to be useful in preliminary design.

Table 3.2 Schmidt Analysis Results

$p = \langle p \rangle \sqrt{1-(a/S)^2}/[(a/S)\cos(\beta+\theta)+1]$	pressure
where	
$\theta = \omega t$	
$a = 0.5\left[(V_{swe}\cos\alpha/T_h + V_{swc}/T_k)^2 + (V_{swe}\sin\alpha/T_h)^2\right]^{1/2}$	
$S = 0.5(V_{swc}/T_k + V_{swe}/T_h) + (V_k + V_{clc})/T_k + V_r\ln(T_h/T_k)/(T_h - T_k) + (V_h + V_{cle})/T_h$	
$\beta = \tan^{-1}\left[(V_{swe}\sin\alpha/T_h)/(V_{swe}\cos\alpha/T_h + V_{swc}/T_k)\right]$	
$W = \pi\langle p \rangle(S/a)[\sqrt{1-(a/S)^2} - 1][V_{swc}\sin\beta + V_{swe}\sin(\beta-\alpha)]$	Work
$Q_c = \pi V_{swc}\langle p \rangle(S/a)[\sqrt{1-(a/S)^2} - 1]\sin\beta$	Heat removed
$Q_e = \pi V_{swe}\langle p \rangle(S/a)[\sqrt{1-(a/S)^2} - 1]\sin(\beta-\alpha)$	Heat added

3.5 Equivalent Alpha Machine for Sinusoidal Motions

In order to use the Schmidt results for beta and gamma machines, it is necessary to reduce these configurations to their equivalent alpha configurations.

The beta and gamma configurations are basically similar except that for the beta arrangement the piston and displacer may have overlapping strokes. Figure 3.8 indicates the piston and displacer motions for both these configurations.

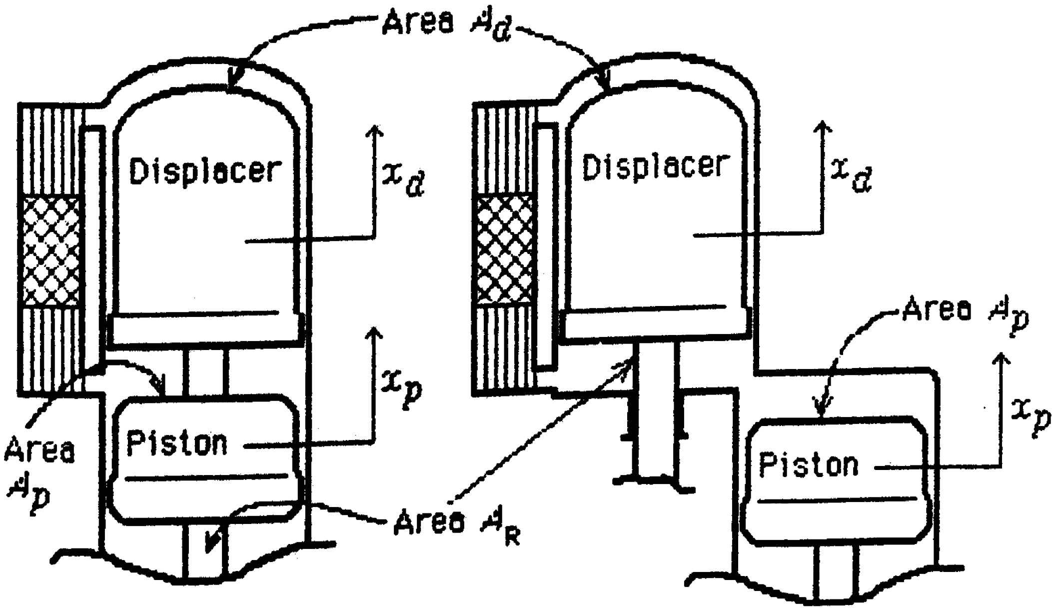

(a) Beta configuration (b) Gamma configuration

Figure 3.8 Piston and Displacer Motions for Beta and Gamma Configurations

The analysis that follows is equally applicable to both beta and gamma configurations.

Referring to Figure 3.8, the expansion space swept volume is given by

$$V_{swe} = 2A_d X_d \tag{3.40}$$

The compression space volume depends on both the piston and displacer motions.

$$V_c = V_{mc} - x_p A_p + x_d(A_d - A_R) \tag{3.41}$$

where A_R is the rod cross sectional area if present and V_{mc} is the mean volume about which the volume variations occur.

For sinusoidal motions, x_p and x_d are given by

$$x_p = X_p \sin\theta \tag{3.42}$$

$$x_d = X_d \sin(\theta + \phi) \tag{3.43}$$

where ϕ is the phase angle by which the displacer motions lead those of the piston.

Substituting (3.42) and (3.43) into (3.41) and simplifying:

$$V_c = V_{mc} + A_pX_p\left[1 - 2(X_d/X_p)(A_d/A_p - A_R/A_p)\cos\phi + \{(X_d/X_p)(A_d/A_p - A_R/A_p)\}^2\right]^{1/2}\sin(\theta - A)$$

where

$$A = \tan^{-1}\left[\frac{-X_d(A_d - A_R)\sin\phi}{-X_pA_p + X_d(A_d - A_R)\cos\phi}\right]$$ (usually in the third quadrant)

V_c may, more conveniently, be written:

$$V_c = (V_{mc} - 0.5\,V_{swc}) + 0.5\,V_{swc}[1 + \sin(\theta - A)]$$

$$= V_{clc} + 0.5\,V_{swc}[1 + \sin(\theta - A)] \tag{3.44}$$

where V_{clc} is the clearance volume and V_{swc} is the swept volume of the compression space and is given by

$$V_{swc} = V_{swp}\sqrt{1 - 2r\cos\phi + r^2} \tag{3.45}$$

where

$V_{swp} = 2A_pX_p$, the swept volume of the piston, and

$r = (X_d/X_p)(A_d - A_R)/A_p$, the reduced displacer to piston stroke ratio.

Generally, in a beta machine $A_d - A_R = A_p$. In this case the stroke ratio is simply:

$$r = X_d / X_p$$

A may also be written in terms of the reduced stroke ratio:

$$A = \tan^{-1}[-r\ \sin\phi/(r\cos\phi - 1)] \tag{3.46}$$

Note that A is the phase displacement of the compression space volume variations behind those of the piston motions. To relate A to the volume phase angle α note that the expansion space volume is in antiphase with the displacer, thus

$$\alpha = \phi - 180° + A \tag{3.47}$$

Figure 3.9 and 3.10 indicate the dependence of V_{swc} and α on ϕ and r. In using these figures, care should be taken to ensure that $V_{mc} \geq 0.5\ V_{swc}$, since otherwise the displacer and piston would foul and their travel will be limited.

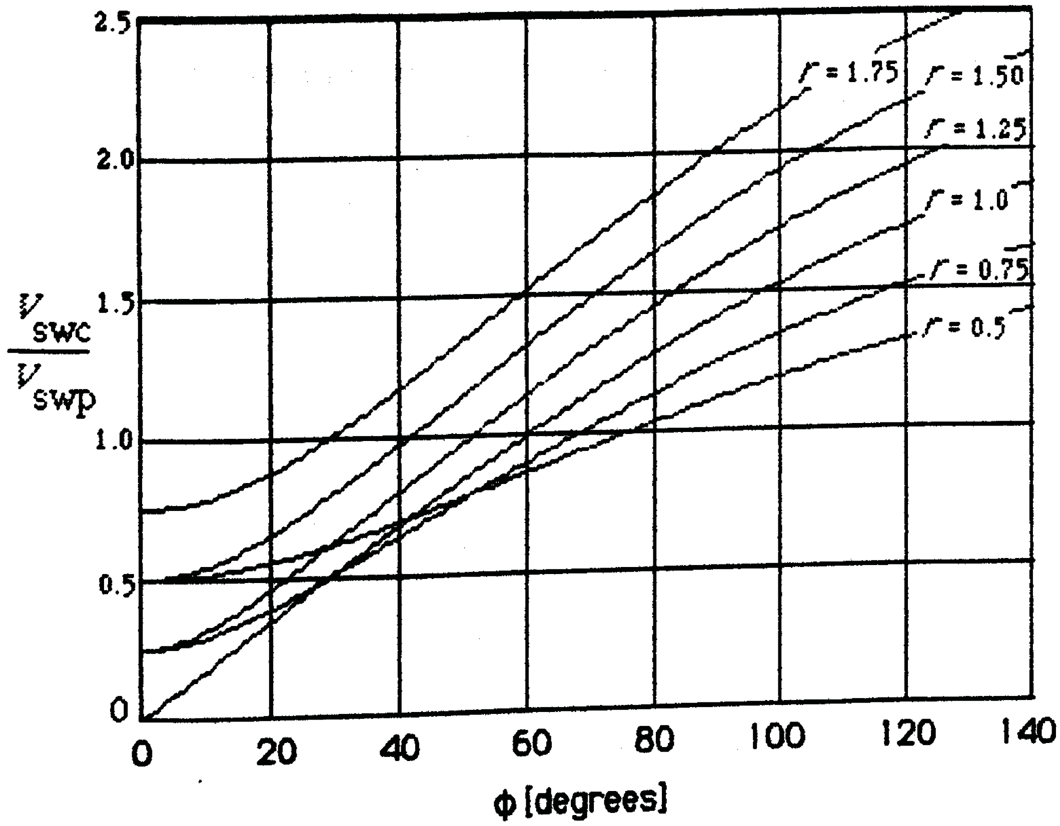

Figure 3.9 Dependence of V_{swc}/V_{swp} on ϕ and r

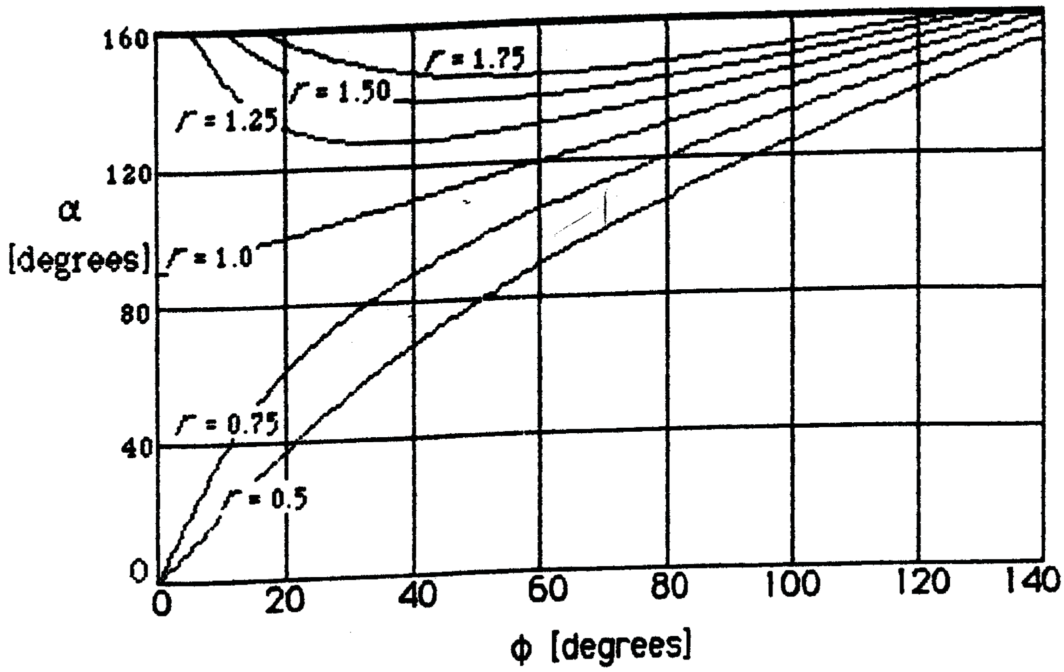

Figure 3.10 Dependence of α on ϕ and r

3.6 Schmidt Solutions in Terms of Displacer and Piston Motions

For beta and gamma machines, particularly free-piston engines, it is often convenient to have the Schmidt solutions in terms of the displacer and piston motions. The procedure for finding these solutions follows in much the same way as outlined for the conventional Schmidt analysis. The details of the mathematics are therefore not presented.

For piston and displacer motions given by

$$x_p = X_p \sin\theta$$

$$x_d = X_d \sin(\theta + \phi),$$

the pressure variation is

$$p = \langle p \rangle \sqrt{1 - (a'/S')^2} \,/\, [(a'/S')\sin(\beta' + \theta) + 1], \tag{3.48}$$

the work on the piston is

$$W_p = 2\pi \langle p \rangle (S'/a')(\sqrt{1 - (a'/S')^2} - 1) A_p X_p \sin\beta' \tag{3.49}$$

and the work on the displacer is

$$W_d = 2\pi \langle p \rangle (S'/a')(\sqrt{1 - (a'/S')^2} - 1) A_R X_d \sin(\beta' + \phi) \tag{3.50}$$

where

$$S' = (V_{mc} + V_k)/T_k + V_r \ln(T_h/T_k)/(T_h - T_k) + (V_{me} + V_h)/T_h$$

$$a' = \Big[[(A_d - A_R)/T_k - A_d/T_h]^2 X_d^2 + 2(A_p/T_k)[(A_d - A_R)/T_k - A_d/T_h] X_d X_p \cos\phi - (A_p X_p/T_k)^2 \Big]^{1/2}$$

$$\beta' = \tan^{-1}\big[\sin\phi/[\cos\phi - (X_p/X_d)\, A_p T_h/\{T_h(A_d - A_R) - A_d T_k\}]\big]$$

where V_{mc} and V_{me} are the mean compression and expansion space volumes respectively.

In the case of a crank machine, the total work delivered to the crank mechanism is $W_p + W_d$. However, in a conventional free-piston machine, the work delivered to the displacer (W_d) is dissipated against viscous losses in the heat exchangers and other irreversibilities and is therefore not recoverable.

A simpler approximate form of W_p and W_d is possible by noting that $a'/S' \ll 1$ and $\sin\beta' = A_d X_d/(T_k a')[1 - T_k/T_h - A_R/A_d]\sin\phi$. Thus expanding the term under the surd sign by binomial series, neglecting higher order terms and simplifying, (3.49) and (3.50) become

$$W_p \approx \pi\langle p\rangle A_p A_d[(1 - T_k/T_h - A_R/A_d)/(T_k S')]X_d X_p \sin\phi \qquad (3.51)$$

$$W_d \approx \pi\langle p\rangle A_R A_p/(T_k S')X_d X_p \sin\phi \qquad (3.52)$$

which shows to a good approximation that the ideal work is directly proportional to X_d and X_p and that it is maximised when the displacer and piston are in quadrature. These observations are not obvious from the Schmidt results based on volumes.

It is instructive to draw a vector diagram for the displacements, volumes and first harmonic of the pressure. Figure 3.11 shows the relative relationships of displacements, volumes and pressure. Note how V_C results

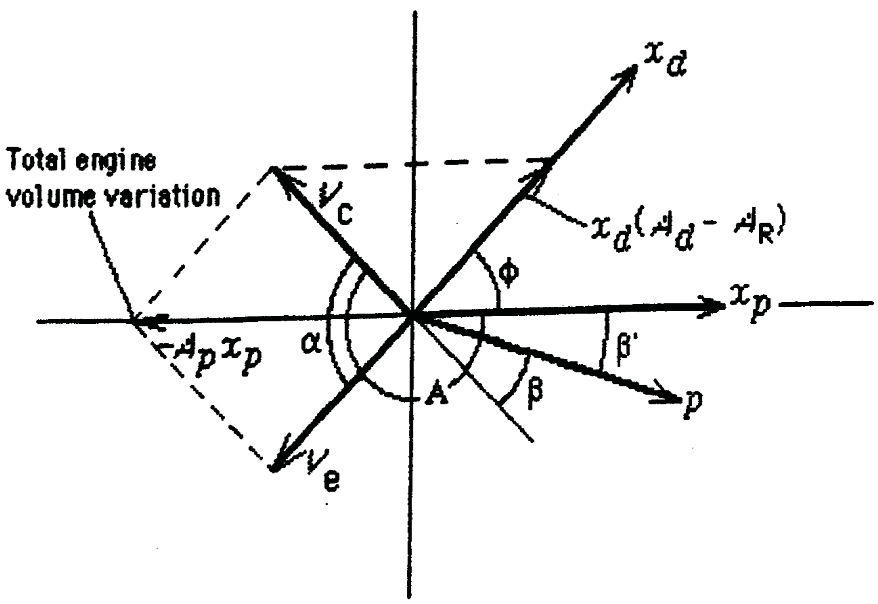

Figure 3.11 Relative Phase Relationships of Displacements, Volumes and Pressure

from components in the directions of the displacer and piston. The pressure is also resolvable into displacer and piston components; this will be further elaborated in Chapter 5. For now note that for positive work the pressure lags the piston motions.

3.7 Simple Optimisation

Walker [Wa73, Wa80] showed that it is possible to non-dimensionalise the Schmidt results by defining three independent variable groups. The groups used here are slightly different from those used by Walker owing mainly to the inclusion of the cooler and heater as separate dead spaces. Also the temperature ratio used here is the inverse of Walker's.

The independent variable groups are as follows:

$\tau = T_h / T_k$	temperature ratio	(3.53a)
$\kappa = V_{swe} / V_{swc}$	swept volume ratio	(3.53b)
$\rho = V_D / V_{swc}$	dead volume ratio	(3.53c)

where

$$V_D = (V_k + V_{clc})(\tau - 1)/\ln\tau + V_r + (V_h + V_{cle})(1 - 1/\tau)/\ln\tau \qquad (3.54)$$

and is referred to as the reduced dead volume. Sometimes V_D is simply taken as the sum of all the unswept volumes. The above definition of V_D more accurately interprets the temperature distribution in the machine.

From Table 3.2, the important results are then:

Non-dimensional cyclic pressure variation:

$$p^* = p/p_{max} = (S^*/a^* - 1)/[\cos(\beta + \theta) + S^*/a^*] \qquad (3.55)$$

Non-dimensional cyclic heat transferred at compression space:

$$Q_c^* = Q_c/(V_t\, p_{max}) = (1 + \kappa)^{-1}\delta\sin\beta \qquad (3.56)$$

Non-dimensional cyclic heat transferred at expansion space:

$$Q_e^* = Q_e/(V_t\, p_{max}) = \kappa(1 + \kappa)^{-1}\delta\sin(\beta - \alpha) \qquad (3.57)$$

Non-dimensional cyclic work:

$$W^* = W/(V_t\, p_{max}) = \delta(1 + \kappa)^{-1}[\sin\beta + \kappa\sin(\beta - \alpha)] \qquad (3.58)$$

Efficiency:

$$\eta = 1 - 1/\tau \qquad (3.59)$$

where p_{max}, V_t, δ, S^*/a^* and β are defined as follows:

$p_{max} = \langle p \rangle \sqrt{1-(a^*/S^*)^2}/[1-(a^*/S^*)]$; the maximum cyclic pressure,

$V_t = V_{swc} + V_{swe}$; the sum of the swept volumes,

$\delta = \pi[(S^*/a^*) - 1][1 - [1-(a^*/S^*)^2]^{1/2}]$,

$S^*/a^* = [\kappa/\tau + 2\rho\ln\tau/(\tau - 1) + 1][(\kappa/\tau)^2 + 2(\kappa/\tau)\cos\alpha + 1]^{-1/2}$ and

$\beta = \tan^{-1}[\sin\alpha/(\cos\alpha + \tau/\kappa)]$

The non-dimensional cyclic work is of particular importance since it indicates the cyclic work for a particular engine size and maximum working gas pressure. The maximum working gas pressure, in turn, gives an indication of the mass of the engine since it determines the thickness of the pressure vessel walls. Consequently, optimising W^* for κ and α given ρ and τ would give the highest power for working gas volume and engine mass. A generalised design chart for optimum W^* is given in Figure 3.12 (taken from [BW79.2]). From the design chart then, given ρ and τ, both κ and α are uniquely defined for maximum W^*. Usually ρ is not known *a prior.* and it is therefore necessary to iterate a few times. As a guide, Table 3.3 lists some ρ's for engines that have been built.

In practical engines, parasitic losses may force an optimised design to be quite different from that suggested by the simple isothermal optimisation. For example, viscous losses will reduce the ideal pV power to some degree. In order to minimise these losses, practical engines operate with low piston-displacer phase angles (usually between 45° and 60°). This translates into a volume phase angle somewhat different from that suggested by Figure 3.12. However, Figure 3.12 still offers a preliminary start on the choice of geometry for a particular engine.

Table 3.3 Dead Volume Ratio for Various Engines

Engine	Source	Volumes ($\times 10^{-6} m^3$)				Temperatures		T_h / T_k	ρ
		V_{swc}	Cooler	Regenerator	Heater	T_h(K)	T_k(K)		
RE-1000	Sunpower	20.6	20.4 (36.7)	56.4	27.3 (17.5)	814	323	2.52	8.72
MAN/MWM	[Wa80]	393	56.5	145.3	100	1023	348	2.94	0.78
GPU-3	[TT79]	114.1	13.1 (26.0)	53.4	47.5 (53.2)	977	288	3.39	1.65
SPIKE-2	Sunpower	176.0	62.1 (217.0)	947.8	162.0 (130.0)	973	310	3.14	9.34
Ford 4-215	[BK77]	218.0	41.1 (53.8)	176.0	128.0 (53.8)	1023	337	3.04	2.11

Volumes thus: ( ) indicate associated clearance volumes.

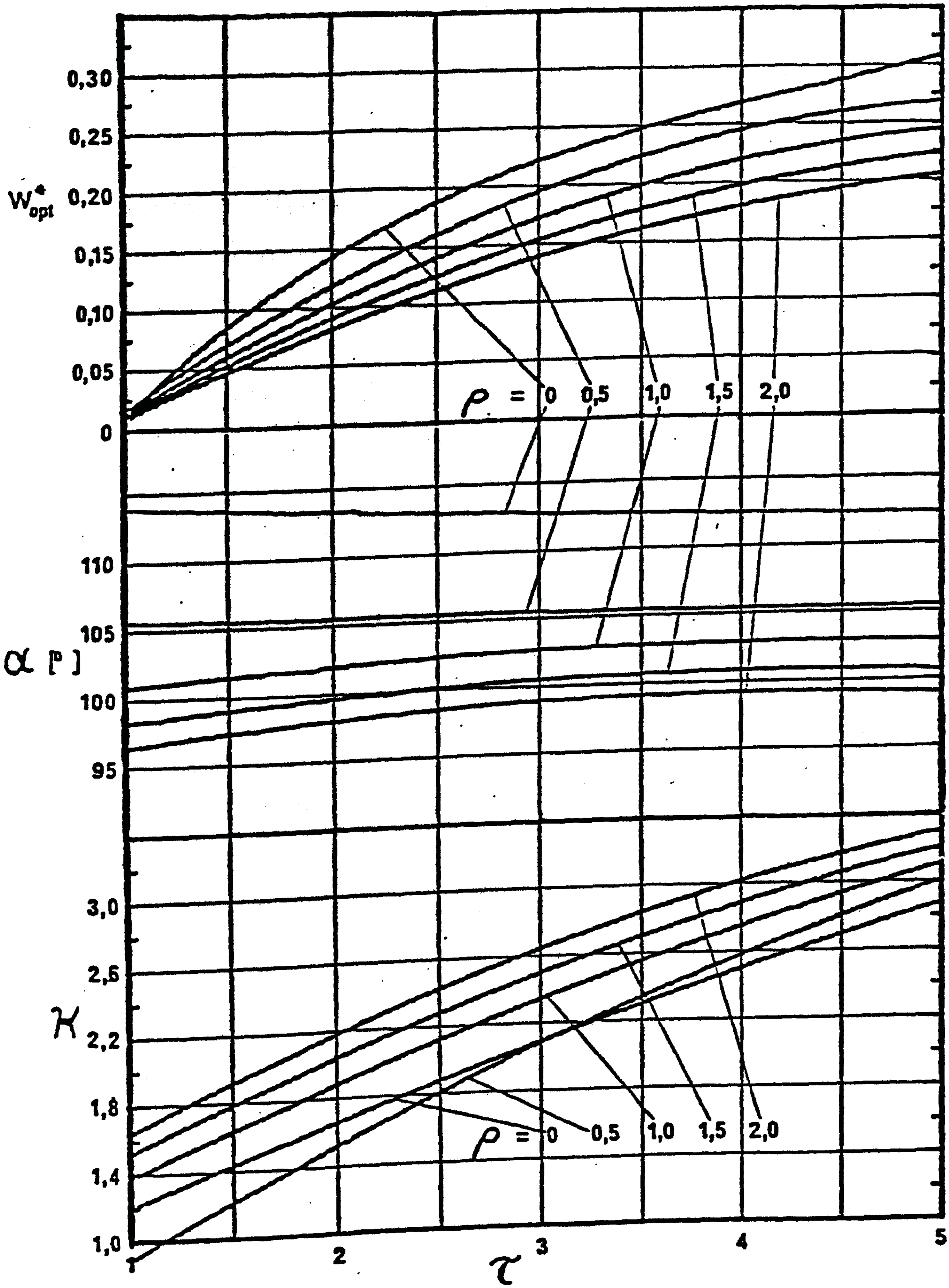

Figure 3.12 Design Chart Based on Schmidt [BW79.2]

3.8 Working Gas Mass Flows

An optimum Stirling engine heat exchanger is one in which for a given transfer of heat, the viscous losses, temperature gradients and internal volume are minimised. The mass flows are required in order to determine the viscous losses and heat transfers (Chapter 4). The Schmidt assumptions allow one to obtain closed-form solutions for the mass flows. These solutions, though simple extensions of the basic Schmidt analysis, have never been presented in the literature. Walker calculated the rate of change of mass in the expansion, compression and dead spaces and inferred qualitatively the mass flows through the heat exchangers [Wa73, Wa80]. Berchowitz derived expressions for the space time distribution of the mass flows for an isothermal machine and compared them to an experimentally validated computer simulation [Be78]. However, both Walker and Berchowitz did not reduce their results to a form which allowed the calculation of the instantaneous mean flow through a particular heat exchanger.

Consider the cooler plus associated dead volume $V_k + V_{clc}$ as in Figure 3.13. From mass continuity over the section up to location x:

$$w_c - w = \mathrm{D}m_x \tag{3.60}$$

From the ideal gas law:

$$\mathrm{D}m_x = A_k x \mathrm{D}p/(RT_k) \tag{3.61}$$

and applying continuity to the compression space:

$$w_c = -Dm_c \tag{3.62}$$

Substituting (3.62) and (3.61) into (3.60):

$$w(x, t) = -A_k x Dp/(RT_k) - Dm_c \tag{3.63}$$

$$0 \leq x \leq L_k$$

which is the time-space mass flow distribution for the cooler.

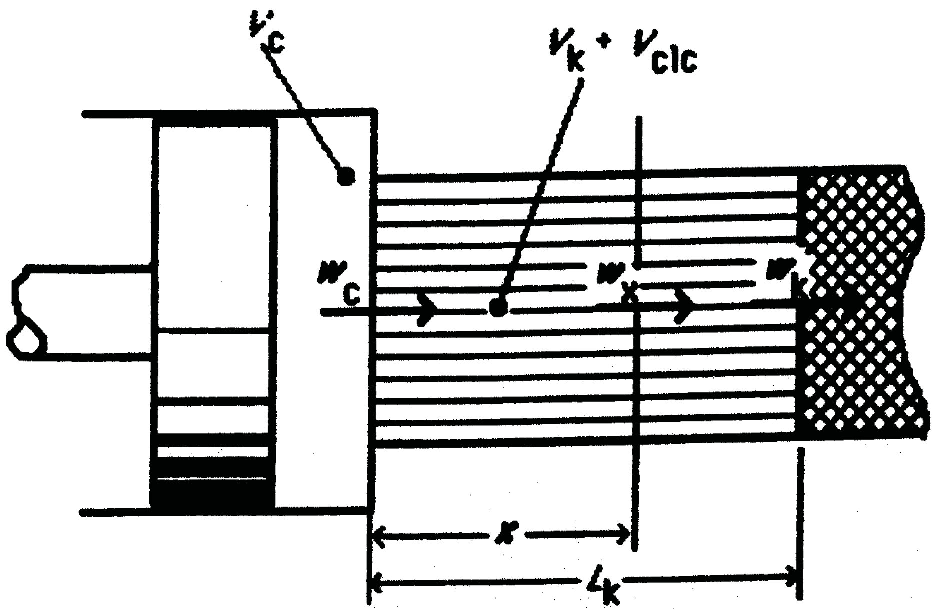

Figure 3.13 Mass Flow in the Cooler

The mean spatial flow rate is defined as follows:

$$\bar{w}_k = L_k^{-1} \int_0^{L_k} w(x, t) dx$$

thus

$$\bar{w}_k = -[(V_k + V_{clc})/2]Dp/(RT_k) - Dm_c$$

and noting that

$$Dm_c = (V_c Dp + pD V_c)/(RT_k)$$

$\bar{w}_k$ becomes

$$\bar{w}_k = -(RT_k)^{-1}\{[(V_k + V_{clc})/2 + V_c]Dp + pD V_c\} \tag{3.64}$$

Substituting for V_c from table 3.1 and for pressure and its derivative from (3.32), the cooler mass flow rate becomes:

$$\begin{aligned}\bar{w}_k = \omega\langle p\rangle(RT_k)^{-1}\{&(V_k + V_{clc} + V_{swc})(S/a)[\sqrt{1-(a/S)^2} - 1]\sin(\beta+\theta)\\ &+ (V_{swc}/2)\sin\theta\\ &+ V_{swc}(S/a)[\sqrt{1-(a/S)^2} - 1]\sin(\beta+2\theta)\\ &+ (V_{swc}/2)\sqrt{1-(a/S)^2}(a/S)^2\sin(2\beta+3\theta)\}\end{aligned} \tag{3.65}$$

since for most practical machines $a/S \ll 1$, (3.65) may be simplified to

$$\bar{w}_k \approx \omega \langle p \rangle (2RT_k)^{-1}\{-(V_k + V_{clc} + V_{swc})(a/S)\sin(\beta+\theta) + V_{swc}\sin\theta$$

$$- V_{swc}(a/S)\sin(\beta + 2\theta)\} \qquad (3.66)$$

where terms containing $(a/S)^2$ and higher order have been neglected.

From (3.65) and (3.66) it is seen that the mass flow has a strong first harmonic and a weaker second harmonic. The third harmonic is of much smaller consequence. If the (a/S) terms are neglected all together, it can then be seen that the mass flow rate through the cooler is almost directly proportional to the volume rate of change in the compression space, but of opposite sign. This observation has been noted empirically by Wood [Wo80].

With the (a/S) terms neglected, $\bar{w}_k$ is given by

$$\bar{w}_k \approx \omega \langle p \rangle (2RT_k)^{-1} V_{swc}\sin\theta \qquad (3.67)$$

Similar results follow for the regenerator and heater.

$$\bar{w}_r = -(RT_k)^{-1}[(V_r'/2 + V_c)Dp + pDV_c]$$

which becomes

$$\bar{w}_r = \omega \langle p \rangle (RT_k)^{-1}\{(V_r' + V_{swc})(S/a)[\sqrt{1-(a/S)^2} - 1]\sin(\beta+\theta)$$

$$+ (V_{swc}/2)\sin\theta$$

$$+ V_{swc}(S/a)[\sqrt{1-(a/S)^2} - 1]\sin(\beta+2\theta)$$

$$+ (V_{swc}/2)\sqrt{1-(a/S)^2}(a/S)^2\sin(2\beta+3\theta)\}$$

where (3.68)

$$V_r' = 2\left\{ V_k + V_{clc} + \frac{V_r}{T_h/T_k - 1}\left[\frac{T_h/T_k \ln(T_h/T_k)}{T_h/T_k - 1} - 1\right]\right\}$$

which for $(a/S) \ll 1$, it can be seen that the regenerator mass flow approaches the phase of the cooler mass flow.

The heater mass flow is

$$\bar{w}_h = -\omega \langle p \rangle (RT_h)^{-1}\{(V_h + V_{cle} + V_{swe})(S/a)[\sqrt{1-(a/S)^2} - 1]\sin(\beta+\theta)$$

$$+ (V_{swe}/2)\sin(\alpha+\theta)$$

$$+ V_{swe}(S/a)[\sqrt{1-(a/S)^2} - 1]\sin(\alpha+\beta+2\theta)$$

$$+ (3V_{swe}/8)\sqrt{1-(a/S)^2}(a/S)^2\sin(\alpha+2\beta+3\theta)\}$$

(3.69)

again for $(a/S) \ll 1$, (3.69) becomes

$$\bar{w}_h \approx \omega \langle p \rangle (2RT_h)^{-1}\{(V_h + V_{cle} + V_{swe})(a/S)\sin(\beta+\theta) - V_{swe}\sin(\alpha+\theta)$$

$$+ V_{swe}(a/S)\sin(\alpha+\beta+2\theta)\} \quad (3.70)$$

and neglecting all (a / S) terms:

$$\overline{w}_h \approx -\omega\langle p\rangle(2RT_h)^{-1}\, V_{swe}\sin(\alpha + \theta) \qquad (3.71)$$

Thus it is clear that the first harmonic of the heater mass flow tends to be almost directly proportional to the volume rate of change of the expansion space. Therefore, for both cooler and heater, the pressure fluctuations do not have a major effect on the mass flow rates through those heat exchangers.

In Figure 3.14 the first harmonics of the cooler and heater mass flows have been added to the phasor diagram of Figure 3.11.

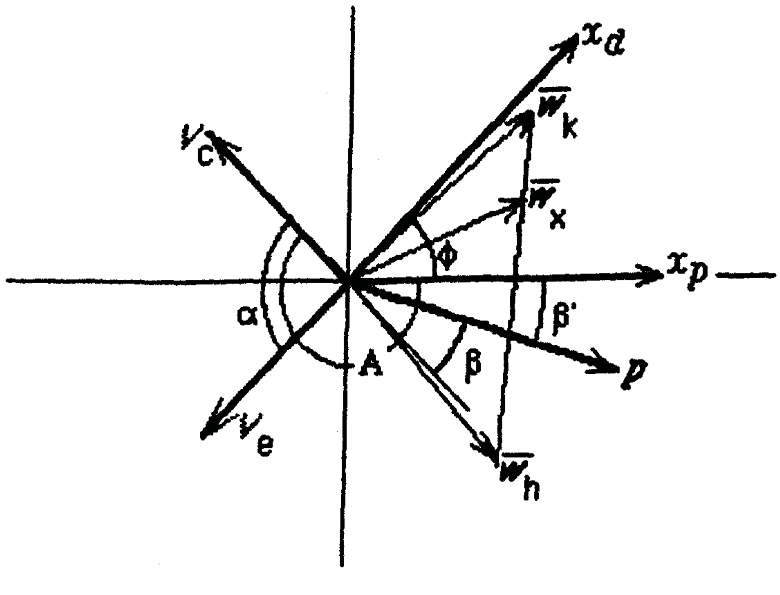

Figure 3.14 Approximate Relative Phase Relationships of Mass Flows, Displacements, Volumes and Pressure

3.9 Utility of the Schmidt Analysis

As has been mentioned before, the primary attraction of the Schmidt analysis is its tractibility and, furthermore, that these solutions have been said to give a fair prediction of performance [Wa80]. It is important to know just how much reliance one can place on the Schmidt results if they are to be truely useful. This is a difficult assessment since the difference between a practical machine and ideal analysis is a complicated function of all the engine parameters.

Martini has estimated that Stirling engines should obtain between 65% and 75% of Carnot for indicated efficiency. He also estimates the indicated power at about 70% of that predicted by Schmidt [Co79]. Walker feels that the indicated efficiency is more likely to fall between 40% and 50% of Carnot [Wa80]. Since the degree with which the Schmidt analysis approaches the actual performance depends on the degree of ideal thermodynamic behaviour, good correlation can only be expected where the non-ideal processes have been minimised. This would be the case for a machine in which great effort has been made to obtain the highest possible efficiency. Obviously an engine with maximised efficiency has minimised irreversibilities. In such circumstances Martini's estimates could probably be approached. However, many applications exist where only moderate efficiencies are required (between 20% and 25% indicated). For example, machines burning rice hulls now being operated in India and Bangladesh are quite competitive with a 10% overall efficiency (the burner efficiency may be only between 50% and 60% thus giving the 10% overall efficiency). In such cases engine irreversibilities are a much larger fraction of the output power and, therefore, not accurately accounting for non-ideal behaviour may result in a machine with performance far short of expectation. Thus if the Schmidt analysis is to be used, due caution should be exercised in estimating the internal losses.

One characteristic of the Schmidt analysis that is not generally recognised is its ability to accurately predict the gas flows within a machine. This is important since together with the heat flows, the heat exchangers may be sized for heat transfer while minimising the viscous losses. The dominant irreversibilities are usually those associated with the heat exchangers.

In practical machines, the spatial pressure drop and the temperature difference between wall and gas are usually small (less than $0.05\langle p \rangle$ and $0.15\langle T \rangle$ respectively). Thus the working gas flow is essentially a function of volume displacements and the local average density. All these parameters are handled by the Schmidt analysis provided that the temperatures used are the mean hot and cold gas temperatures. The temperatures intuitively obvious are the volumetric means which from experience seem to give the best overall correlation. The volumetric mean temperature is defined as follows:

$$\langle T \rangle_v = (T_{sw} V_{sw} + T_{exc} V_{exc})/(V_{sw} + V_{exc}) \qquad (3.72)$$

where

T_{sw} is the mean swept volume temperature,

T_{exc} is the mean heat exchanger temperature,

V_{sw} is the associated swept volume and

V_{exc} is the associated heat exchanger volume.

Figure 3.15 compares the mass flows between the ideal adiabatic analysis (Appendix C) and the Schmidt analysis for the RE-1000 (the RE-1000 is a free-piston research engine developed at Sunpower Inc - see Appendix A). It can be seen that even in the extreme case of adiabatic working spaces, the Schmidt analysis predicts the mass flows fairly well. There is a phase difference of about 30° whereas the amplitudes are similar. For calculating the viscous dissipation losses in the heat exchangers, the error in the phase relationship is not significant. However, this error must be kept in mind when calculating the damping on a free-piston displacer since displacer damping is often critical in obtaining correct free-piston engine dynamics. The approximate calculations (Equations (3.67) and (3.71)) of the mass flows for the RE-1000 are shown in Figure 3.16. Here the agreement is a little poorer but still representative.

Other areas of reasonably good prediction are the pressure variations [Be78] and the regenerator heat rate as was already shown in Figure 3.5.

Knowing the required heat transfer, the mass flows and the regenerator heat rate allows one to begin preliminary optimisation of the heat exchangers.

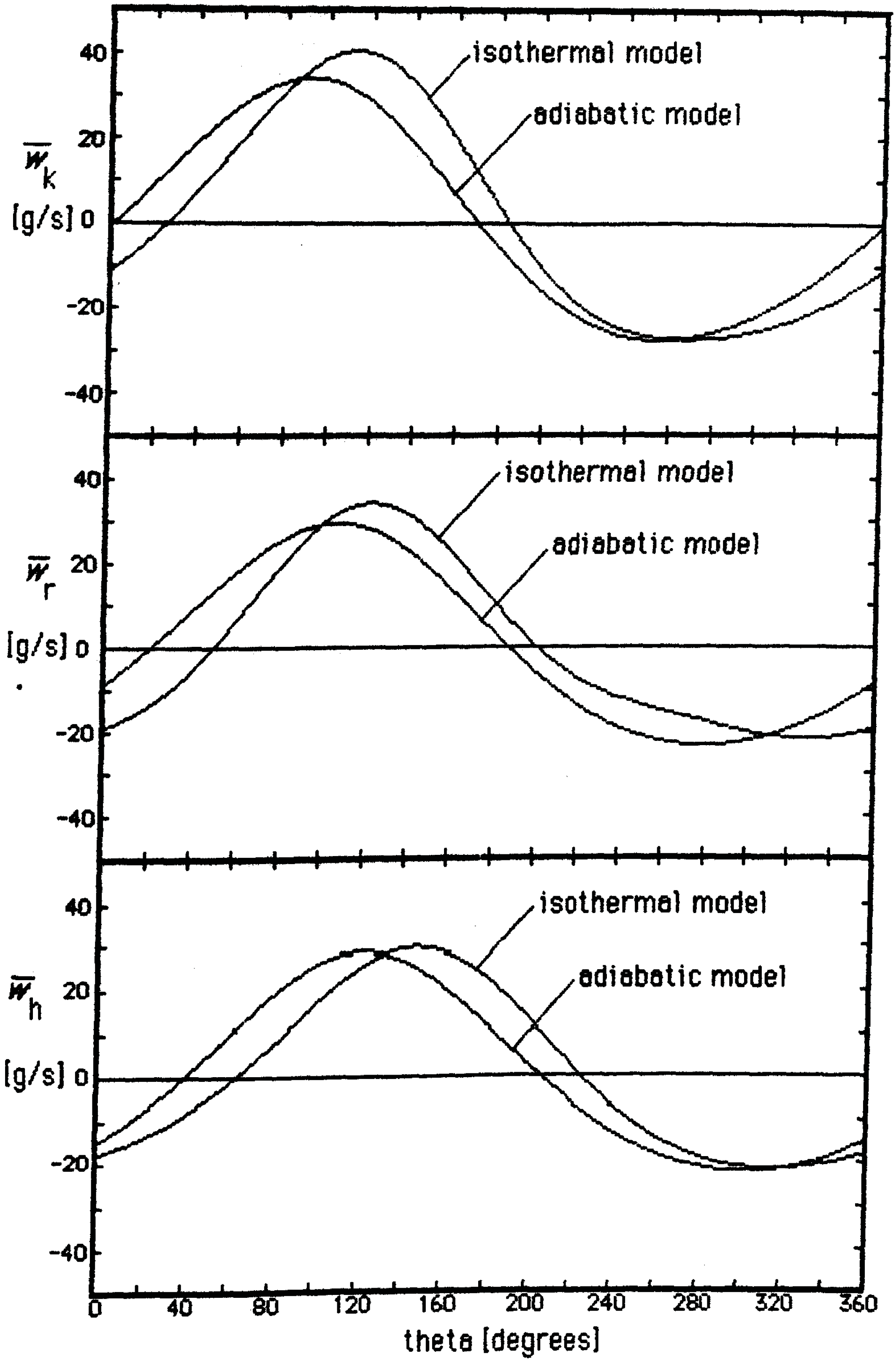

Figure 3.15 Mass Flows vs Theta for RE-1000

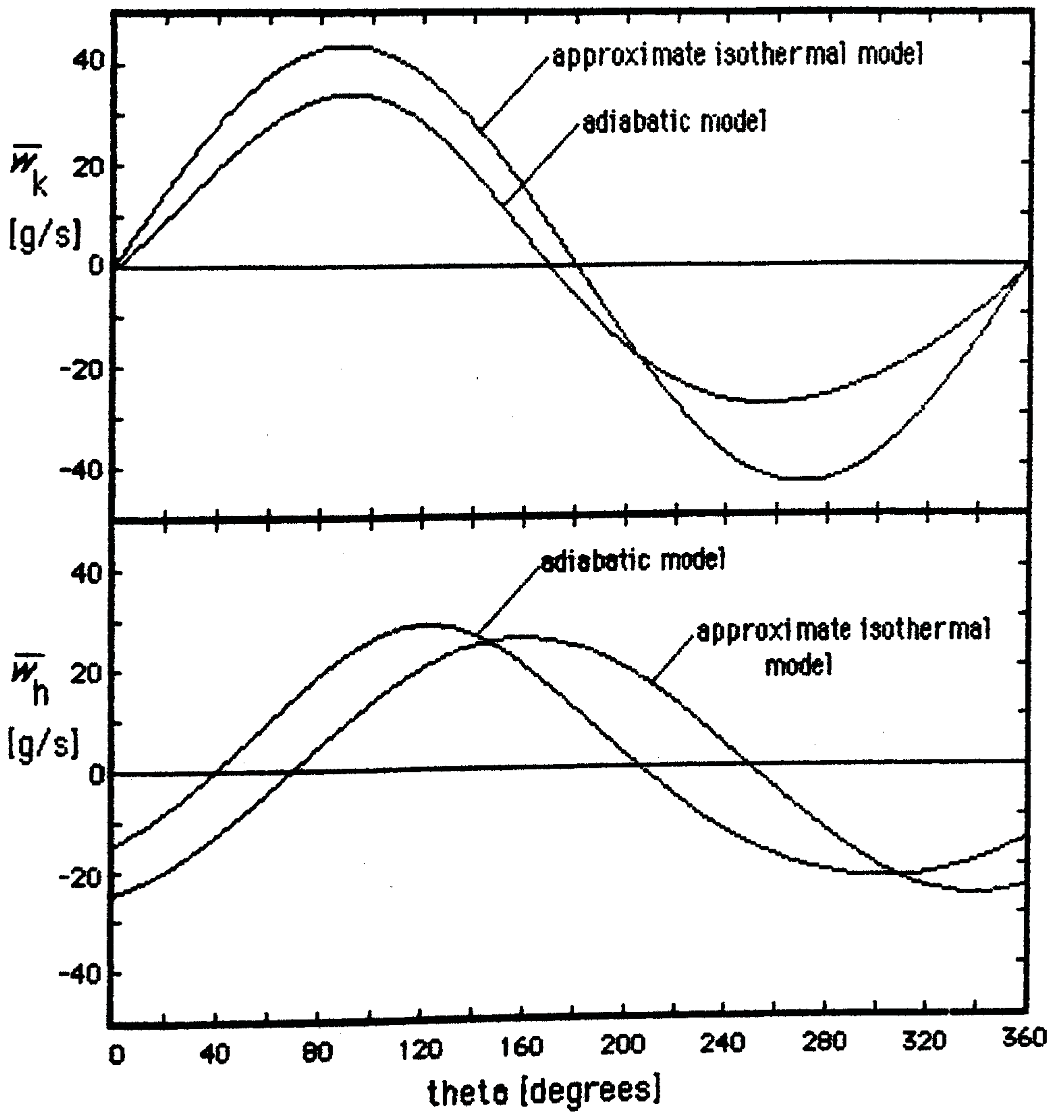

Figure 3.16 Approximate Mass Flows for RE-1000